

G Arnoux, I. Balboa, M. Clever, S. Devaux, P. De Vries, T. Eich, M. Firdaouss,
S. Jachmich, M. Lehnen, P.J. Lomas, G.F. Matthews, Ph. Mertens, I. Nunes,
V. Riccardo, C. Ruset, B. Sieglin, D.F. Valcarcel, J. Wilson, K.-D. Zastrow
and JET EFDA contributors

Power Handling of the JET ITER-Like Wall

Power Handling of the JET ITER-Like Wall

G Arnoux¹, I. Balboa¹, M. Clever², S. Devaux³, P. De Vries⁴, T. Eich³, M. Firdaouss⁵,
S. Jachmich⁶, M. Lehnen², P.J. Lomas¹, G.F. Matthews¹, Ph. Mertens³, I. Nunes⁷,
V. Riccardo¹, C. Ruset⁸, B. Sieglin³, D.F. Valcarcel⁸, J. Wilson¹, K.-D. Zastrow¹
and JET EFDA contributors*

JET-EFDA, Culham Science Centre, OX14 3DB, Abingdon, UK

¹*EURATOM-CCFE Fusion Association, Culham Science Centre, OX14 3DB, Abingdon, OXON, UK*

²*Forschungszentrum Jülich, Institute of Energy Research - Plasma Physics,
EURATOM Association, D-52425, Jlich, Germany*

³*Max-Planck-Institut für Plasmaphysik, EURATOM-Assoziation, 85748 Garching, Germany*

⁴*FOM Institute DIFFER P.O. Box 1207 NL-3430 BE Nieuwegein, The Netherlands*

⁵*Association EURATOM-CEA, CEA/DSM/IRFM, Cadarache 13108 Saint Paul Lez Durance, France*

⁶*Association "EURATOM - Belgian State" Laboratory for Plasma Physics Koninklijke Militaire School
- Ecole Royale Militaire Renaissancelaan 30 Avenue de la Renaissance B-1000 Brussels Belgium*

⁷*Associação EURATOM/IST, Instituto de Plasmas e Fusão Nuclear, Instituto Superior Técnico,
Av Rovisco Pais, 1049-001 Lisbon, Portugal*

⁸*National Institute for Laser, Plasma and Radiation Physics, Association Euratom-MedC, Bucharest, Romania*

** See annex of F. Romanelli et al, "Overview of JET Results",
(24th IAEA Fusion Energy Conference, San Diego, USA (2012)).*

Preprint of Paper to be submitted for publication in Proceedings of the
14th International Conference on Plasma-Facing Materials and Components for Fusion Applications,
Jülich, Germany.
13th May 2013 - 17th May 2013

“This document is intended for publication in the open literature. It is made available on the understanding that it may not be further circulated and extracts or references may not be published prior to publication of the original when applicable, or without the consent of the Publications Officer, EFDA, Culham Science Centre, Abingdon, Oxon, OX14 3DB, UK.”

“Enquiries about Copyright and reproduction should be addressed to the Publications Officer, EFDA, Culham Science Centre, Abingdon, Oxon, OX14 3DB, UK.”

The contents of this preprint and all other JET EFDA Preprints and Conference Papers are available to view online free at www.iop.org/Jet. This site has full search facilities and e-mail alert options. The diagrams contained within the PDFs on this site are hyperlinked from the year 1996 onwards.

ABSTRACT.

The ITER-like wall (ILW) at JET is a unique opportunity to study the combination of material (beryllium and tungsten) that will be used for the plasma facing components (PFC) in ITER. Both the limiters (Be) and divertor (CFC W coated and bulk W) have been designed to maximise their power handling capability. During the last experimental campaign (October 2010 to July 2011) this capability has been assessed and even challenged in the case of the beryllium wall.

The Be limiters are composed of highly shaped, castellated tiles. They are optimised for a range of scrape-off-layer (SOL) power decay length $5 < \lambda_{q,\text{design}} < 20\text{mm}$. Its power handling capability ($19\text{MW}/\text{m}^2\text{s}^{1/2}$), predicted with a simple model, has been proven to be robust by the experiments despite unexpected power loads pattern. However, this capability has been pushed to its limit leading to Be melt events, which revealed that the power load is toroidally asymmetric. The toroidal asymmetry could be explained by a misalignment of the limiters by 1mm.

The protection system of the ILW has now been partially commissioned and the main chamber protection was operational. It did not prevent melt events mainly because the protection The bulk W divertor target performed as predicted. Operations were constrained by: 1) an energy load limit of 60MJ per stack ($60\text{MJ}/\text{m}^2$), and 2) the limited number of cycles of the surface temperature above 1200°C in order to prevent thermal fatigue.

This latter limit has been exceeded about 300 times and no signs of damage or thermal fatigue have been observed by the photogrammetric survey.

1. INTRODUCTION

The ITER-like wall at JET is made of the same combination of plasma facing materials that is foreseen for the active operation in ITER: beryllium for the first wall and tungsten in the divertor. The ITER-like wall is a unique opportunity to test the power handling capability of the different plasma facing components (PFCs) under relevant heat loads conditions due to plasma wall interaction.

Be has a melting temperature of 1257°C , which typically is reached in 10s with a heat load of $6\text{MW}/\text{m}^2$. The W has a much higher melting temperature ($T_{\text{melt}} = 3422^\circ\text{C}$) but is rather brittle and get weaker under thermal stresses (thermal fatigue). Thermal cycle above 1200°C must be budgeted to allow for a reasonable life time of the components [1]. In JET only the divertor outer, horizontal target is made of bulk W. The remaining PFCs in the divertor are made of CFC W coated tiles. Previous R & D activities showed that the risk of delamination of the coating is very small if the temperature is kept below 1200°C . The design of the ITER-like wall was mainly driven to optimise the PFCs power handling capability, thereby minimising the constraints on the plasma operations. There is one major difference in JET compared to ITER: the JET plasma facing components are all inertially cooled.

The PFC power handling capability, constrained by material limits depends on the expected power loads from the plasma flux. Given the total power entering the scrape-off-layer (SOL), P_{SOL} , one can in principle predict the power distribution, $q_{\text{PFC}} [\text{MW}/\text{m}^2]$, and thereby the peak heat load,

q_{pk} [MW/m²], onto the PFCs. The expected power load distribution is usually predicted assuming a known parallel heat flux profile in the SOL, $q_{||}(r_{mid})$, defined at the outer mid-plane (r_{mid} is the outer mid-plane radius). It is assumed that heat perpendicular transport is poloidally symmetric and dominated by diffusion such that $q_{||}(r_{mid}) = q_{0||} \cdot \exp[-r_{mid}/\lambda_q]$, where $\lambda_q = q/\nabla q$ is the SOL power decay length. The properties at the outer mid-plane (upstream) are then projected along the field lines down to the PFCs assuming toroidal symmetry.

An important feature of the PFC design is to avoid leading edges. The field line angles onto the PFC surface usually is rather shallow, typically $80^\circ < \theta_n < 89^\circ$, where $\cos(\theta_n) = |\mathbf{B} \cdot \hat{\mathbf{n}}|$ with \mathbf{B} , the magnetic field and $\hat{\mathbf{n}}$, the normal vector to the PFC surface. The heat load onto the PFC surface is determined by: $q_{PFC;surf} = \cos(\theta_n) \cdot q_{||;PFC}$, where $q_{||;PFC}$ is the parallel heat flux at the PFC location. Any gap between surfaces potentially have field lines reaching an edge orthogonal to the surface, which yields $q_{PFC;edge} = \sin(\theta_n) \cdot q_{||;PFC}$. The heat loads onto a leading edge can therefore be much higher than that on the surface: $10 < q_{PFC;edge} = q_{PFC;surf} = \tan(\theta_n) < 30$. Particular attention has been put in the design in order to shadow any leading edges.

This paper will review the different models used to predict the heat loads distribution onto the PFCs and compare with the measurements made in dedicated experiments. In section 2, we discuss the power handling of the first wall and why the protection system of the ITER-like wall (PIW) did not prevent melt events when we challenged its power handling capability. In section 3, we discuss the power handling capability of the bulk W. The CFC W coated components have not received significant heat loads during the last experimental campaign and inspections revealed few, very localised, signs of delamination but nothing systematic.

2. BERYLLIUM FIRST WALL

The first wall is composed of castellated Be tiles [2] highlighted in green in Figure 1. Other components of the first wall are made of Inconel or CFC with a coating of either beryllium (cyan) or tungsten (magenta) but will not be discussed in this paper as they are barely exposed to plasma loads (They are recessed with respect to the bulk Be poloidal limiters by at least 40mm). The inner and outer wall is composed of discrete, unevenly distributed poloidal limiters. The outer poloidal limiters (OPL) and inner wall guard limiters (IWGL) are composed of 24 and 19 tiles respectively. The detailed tile assemblies of the IWGL and wide OPL are shown in Figure 1. Those are the key PFCs of the first wall and we will focus mainly on the inner limiter since it is where the plasma starts-up and terminates most of the time. The first wall at the top of the machine is composed of 64 rows of 8, roof shaped tiles (upper dump plates) and of 20 pair of cylindrically shaped tiles (upper inner protections). Those will be discussed at the end of this section as they are important during transients power loads resulting from uncontrolled plasma terminations (disruptions).

The inner wall tiles were designed to minimise the peak heat load onto the limiter for SOL power decay length in the range: $5 \leq \lambda_q \leq 20\text{mm}$ (defined at the outer mid-plane). A map of the heat flux deposited onto the IWGL 8Z, predicted by the 3D field line tracing and heat flux calculation code

PFCFLUX [3], is shown in Figure 2 (a) and (b) for $\lambda_q = 5$ and 20mm respectively. In both cases the magnetic equilibrium comes from the same experiment - JET Pulse number (JPN) 80836- in which $P_{\text{SOL}} = 1.54\text{MW}$. It clearly shows that a shorter λ_q concentrates the heat load closer to the plasma contact point. In both cases the peak heat load remains located near the wings of the limiter but the profile is flatter when $\lambda_q = 5\text{mm}$. A realistic prediction of the heat load distribution can only be obtained if one takes into account shadowed areas (in dark blue in Figure 2 (c)) from the other limiters. By definition in the code a shadowed area receives no heat flux if it is not connected to the outer mid-plane. In our specific case, an area is considered wetted if the field lines, starting from the limiter, do not intersect another PFC after 30m (the connection length between the contact point and the outer mid-plane is 25m). This is of course a simplified view and a comparison with the measurements (Figure 2 (d)), derived from the images taken with a wide angle, medium wavelength infrared (MWIR, $4\mu\text{m}$) camera [4], shows that the reality is slightly more complex than what the model predicts. A comparison between the measurements and the model of two poloidal (vertical) profiles (Figure 2 (e) and (f) respectively) leads to one conclusion: the measured peak value ($q_{\text{p||;meas}} \approx 0.5\text{MW/m}^2$ on the ridge) is about 2 times lower than that predicted by the code ($q_{\text{p||;pred}} \approx 1\text{MW/m}^2$ on the wing) and is not at the same location. Our model is therefore rather conservative since it overestimates the peak heat load. The fact that we measure the peak heat load onto the limiter ridge, exactly at the plasma contact point rather than on the wings is not yet fully understood and is discussed in details in [5]. Note that $q_{\text{||}}(r_{\text{mid}})$ inferred from the IR measurements is such that q/∇ is not constant, with a much steeper gradient in the near SOL. This means that the SOL width cannot be described with a single λ_q . On the OPL the difference between the model and the measurements is smaller and absolute values of heat loads are in much better agreement.

The inner wall was challenged during a dedicated experiment (JET Pulse No: 83620) where $P_{\text{SOL}} = 4.7\text{MW}$ (to be compared with 1.54MW in our previous example), applied for about 8s using 5MW of neutral beam heating power. This experiment was relying on the protection system of the ITER-like wall (PIW) which safely stops the plasma pulse if an overheating of the wall is detected [6]. The peak heat load measured on the IWGL 8Z is $q_{\text{p||;meas}} = 3\text{MW/m}^2$, leading to a maximum $T_{\text{peak}} \sim 1000^\circ\text{C}$ (see MWIR measurement in Figure 3), far from melt temperature, even taking into account uncertainties (100°C at 1000°C). However, an inspection showed strong melts on the ridge of the neighbour limiter (IWGL 8X) (see picture in Figure 3) [7], which coincides with the plasma contact point. A comparison of T_{peak} measured on the IWGL 8Z and 8X using the protection cameras (NIR) indicate that there is a strong toroidal asymmetry of the power load onto the limiter. Using T_{peak} from the NIR camera we estimate that $q_{\text{p||}} \approx 6\text{MW/m}^2$ on the IWGL 8X. This could be explained by a 1mm misalignment of the limiters if $q/\nabla q = 5\text{mm}$ in the near SOL, which is realistic. A systematic inspection of the inner wall revealed that 4 limiters were strongly melted, 4 limiters had shallow melts (See example in Figure 3) and 8 limiters were intact. The protection system did not prevent melting because it was monitoring the IWGL 8Z only and assumed toroidal symmetry. In the next campaign the PIW cameras will monitor 4 IWGL.

During disruptions, the amount of energy (thermal and magnetic) dissipated by radiation is about two times smaller with the ILW (10% of the total energy in average) than it was with the JET carbon wall [8]. The energy driven by the plasma to the wall is therefore much larger and led to systematic melts on the 96 rows of the upper dump plate and upper inner protections. Mitigation of these thermal loads by massive gas injection of a mixture of deuterium and argon is now mandatory for plasmas operating at plasma current $I_p \geq 2.0\text{MA}$.

3. TUNGSTEN DIVERTOR

The divertor horizontal, outer target is composed of 48 pairs of tiles. Each tile assembly (Figure 1) is composed of 4 stacks, each stack being made of 24 lamellas approximately 6mm wide (toroidal direction), 60mm long (poloidal direction) and 40mm deep. Compared to the former CFC outer target, where each tile was made of a single block, this design is less efficient to diffuse the heat into the tile volume. Since the plasma heat load is mainly localised on one stack, the heat diffuses down the to the tile carrier much more quicker. The tile carrier is made of Inconel which has a temperature limit of 600°C. The lamellas are mounted on the Inconel wedges and pre-loaded using springs at the back of the wedges, which have a temperature limit of 330°C and are therefore the weakest part of the tile assembly. According to the GTM model, which has been validated on the Marion facility [9], this limit imposes that no more than 60MJ can fall on a stack, which typically corresponds to a total energy onto the outer target of 74MJ and a total energy into the SOL of 111MJ (assuming a divertor power load asymmetry: $P_{\text{div},\text{in}}/P_{\text{div},\text{out}} = 1/2$) [1]. This is too restrictive from the plasma scenario point of view and a strike point sweeping is necessary to spread the heat load over more than one stack. This method has been used very successfully in the last JET campaigns.

The predictions of the GTM model have been compared with measurements in dedicated experiments with moderate input power ($P_{\text{heat}} \leq 15\text{MW}$). The measurements of the tile surface temperature is made using IR thermography [10] and the temperature at the back of the lamellas, on the wedges (tile carrier) and on the springs was measured by thermocouples (Figure 4 (b)). The measured temperature increase, ΔT_{meas} is compared to the GTM predictions, ΔT_{pred} , in Figure 4 (a) for different stacks (C and D) and different measurement positions. It shows that ΔT_{meas} at the surface is higher by up to 50% than that predicted. On the other hand, ΔT_{meas} in the carrier and spring are lower. One could conclude that the diffusion to the tile carrier is less efficient than expected (lower thermal contact), which is positive in term of tile carrier protection. However that indicates that operations are slightly more restricted if one wants to avoid thermal fatigue, since high surface temperatures are reached quicker than expected. Note that for the GTM model, the global wetted fraction: $\text{GWF} = 1$, whereas in reality $0.7 \leq \text{GWF} \leq 0.8$ (depending on the safety factor) as illustrated by the IR image in Figure 4 (b). This could also explain the higher measured ΔT_{surf} since a lower GWF means a higher peak heat load for the same P_{SOL} . This will be verified with deeper analysis of our measurements. The IR image in Figure 4 shows that leading edges are properly shadowed. Slight non uniformity of the heat load on lamellas is the results of small vertical misalignment

($\Delta z \leq 120\mu\text{m}$), which is well below the tolerances of the design ($\Delta z_{\text{max}} = 400\mu\text{m}$). Overall, the divertor target went about 300 times above 1200°C and no sign of thermal fatigue have been identified.

4. CONCLUSION

The power handling capability of the JET ITER-like wall has been tested experimentally and met the expected performance despite small differences between the measurements and the predictions of our models. The model used for the first wall proved to be robust since it overestimates the peak power load. The measured peak power load systematically coincides with the plasma contact point, which is not predicted by the model. This can't be a measurement artefact since it is where molten beryllium was observed when the wall was challenged at high power. The molten Be revealed that the power load is not toroidally symmetric, and this must be taken into account in the first wall protection strategy. The measurements in the divertor indicate that the thermal contact between the tungsten and the tile carrier is lower than that in the model, leading to higher surface temperature than expected. Surface temperature measurement on both the first wall and the divertor showed that the leading edges are properly shadowed.

ACKNOWLEDGEMENT

This work, supported by the European Communities under the contract of Association between EURATOM and CCFE, was carried out within the framework of the European Fusion Development Agreement. The views and opinions expressed herein do not necessarily reflect those of the European Commission. This work was also part-funded by the RCUK Energy Programme under grant EP/I501045.

REFERENCES

- [1]. Ph. Mertens, J.W. Coenen, T. Eich, A. Huber, S. Jachmich, D. Nicolai, V. Riccardo, K. Senik, U. Samm, and JET-EFDA Contributors. Power handling of a segmented bulk W tile for JET under realistic plasma scenarios. *Journal of Nuclear Materials*, **415**:S943–S947, 2011.
- [2]. V. Riccardo, P.J. Lomas, G.F. Matthews, I. Nunes, V. Thompson, E. Villedieu, and JET-EFDA Contributors. Design, manufacture and initial operation of the beryllium components of the JET ITER-like wall. *Fusion Engineering and Design*, In Press(<http://dx.doi.org/10.1016/j.fusengdes.2013.01.084>), 2013.
- [3]. M. Firdaouss, V. Riccardo, V. Martin, G. Arnoux, and JET-EFDA Contributors. Modelling of power deposition on the JET ITER-like wall using the code PFCFLUX. *Journal of Nuclear Materials*, (In press), 2013.
- [4]. E. Gauthier, H. Roche, E. Thomas, S. Droineau, B. Bertrand, J.B. Migozzi, W. Vliegthart, L. Dague, P. Andrew, T. Tiscornia, and JET-EFDA Contributors. ITER-like wide angle infrared thermography and visible observation diagnostic using reflective optics. *Fusion Engineering and Design*, **82**:1335–1340, 2007.

- [5]. G. Arnoux, T. Farley, C. Silva, S. Devaux, M. Firdaouss, D. Frigione, R.J. Goldston, J. Gunn, J. Horacek, S. Jachmich, P.J. Lomas, S. Marsen, G.F. Matthews, R. A. Pitts, M. Stamp, P.C. Stangeby, and JET-EFDA Contributors. Scrape-off-layer properties of ITER-like limiter startup plasmas in JET. *Nucl. Fusion*, (Accepted for publication), 2013.
- [6]. G. Arnoux, S. Devaux, D. Alves, I. Balboa, C. Balorin, N. Balshaw, M. Belsishevsky, P. Carvalho, M. Clever, S. Cramp, J.-L. de Pablos, E. de la Cal, D. Falie, P. Garcia-Sanchez, R. Felton, V. Gervaise, A. Goodyear, A. Horton, S. Jachmich, A. Huber, M. Jouve, , D. Kinna, U. Kruezi, A. Manzanares, V. Martin, P. McCullen, V. Moncada, K. Obrejan, K. Patel, P.J. Lomas, A. Neto, F. Rimini, C. Ruset, B. Schweer, G. Sergienko, B. Sieglin, A. Soletto, M. Stamp, A. Stephen, P.D. Thomas, D.F. Valcarcel, J. Williams, J. Wilson, K.-D., and JET-EFDA Contributors. A protection system for the JET ITER-like wall based on imaging diagnostics. *Review of Scientific Instruments*, **83**:10D727, 2012.
- [7]. G. Sergienko, G. Arnoux, S. Devaux, G.F. Matthews, I. Nunes, V. Riccardo, A. Sirinelli, A. Huber, S. Brezinsek, J.W. Coenen, Ph. Mertens, V. Philipps, U. Samm, and JET-EFDA Contributors. Movement of liquid beryllium during melt events in JET with the ITER-like wall. Proc. in 14th conference on plasma facing material (PFMC), Juelich, Germany, (A104), 2013.
- [8]. M. Lehnen, G. Arnoux, S. Brezinsek, J. Flanagan, S.N. Gerasimov, N. Hartmann, T.C. Hender, A. Huber, S. Jachmich, U. Kruezi, G.F. Matthews, J. Morris, V.V. Plyusnin, C. Reux, V. Riccaardo, B. Sieglin, P.C. de Vries, and JET-EFDA Contributors. Impact and mitigation of disruptions with the ITER-like wall in JET. Proc. in 24th IAEA Fusion Energy Conference, San Diego, USA, (EX/9-1), 2012.
- [9]. Ph. Mertens, H. Altmann, P. Chaumet, E. Jorin, M. Knaup, G.F. Matthews, O. Neubauer, D. Nicolai, V. Riccardo, V. Tanchuk, V. Thompson, R. Uhlemann, and U. Samm. A bulk tungsten tile for jet: Heat flux tests in the MARIONS facility on the power-handling performance and validation of the thermal model. *Fusion Engineering and Design*, **86**:1801–1804, 2011.
- [10]. I. Balboa, G. Arnoux, T. Eich, B. Sieglin, S. Devaux, W. Zeidner, C. Morlock, U. Kruezi, G. Sergienko, D. Kinna, P.D. Thomas, M. Rack, and JET-EFDA Contributors. Upgrade of the infrared camera diagnostics for the JET ITER-like wall divertor. *Review of Scientific Instruments*, **83**:10D530, 2012.

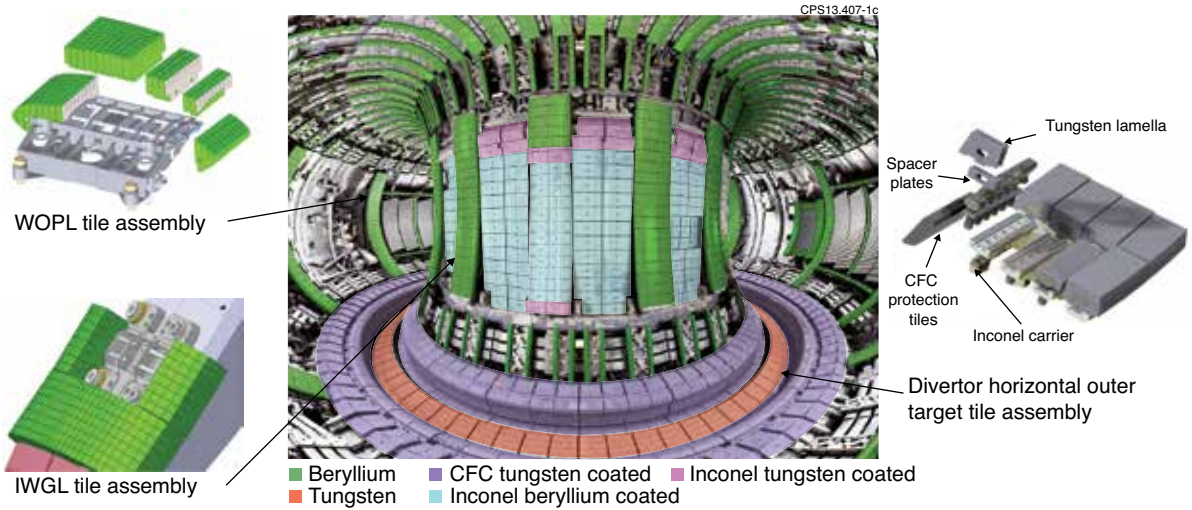


Figure 1: Overview of the JET ITER-like wall plasma facing components. The first wall (green, cyan and magenta) is mainly composed of bulk beryllium, beryllium coated or tungsten coated tiles. The coated tiles are either made of CFC or Inconel. The divertor (red and purple) is composed of bulk tungsten or CFC tungsten coated tiles. The details of the tile assembly are shown for the wide outer poloidal limiter (WOPL), the inner wall guard limiter (IWGL) and the divertor horizontal, outer target (bulk W).

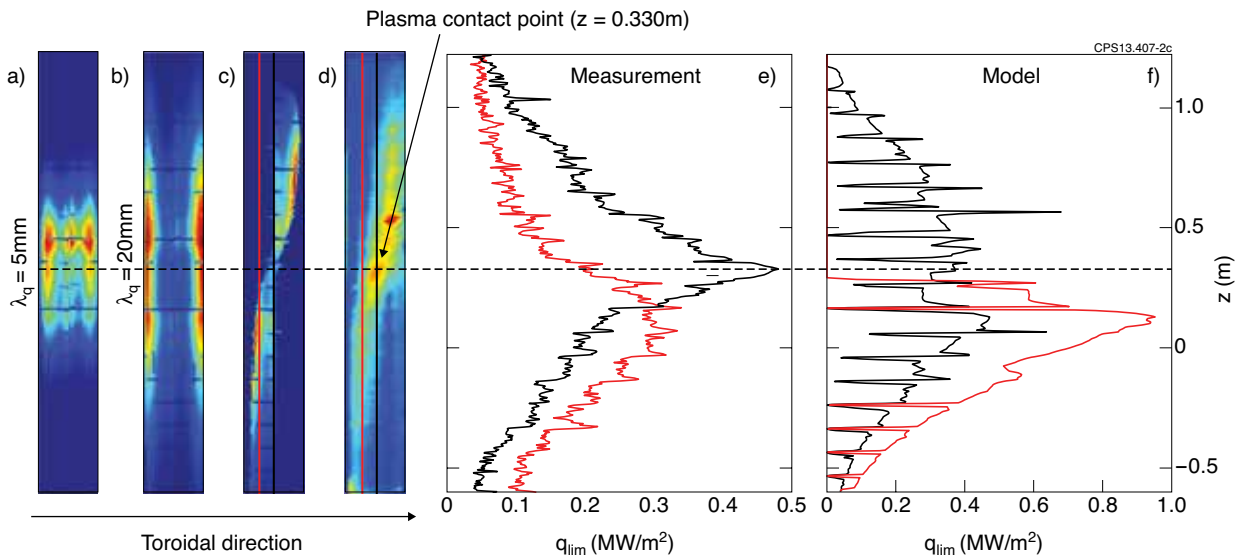


Figure 2: Heat flux map on the IWGL predicted with PFCFLUX (a) without and (b) with shadowing. (c) heat flux map derived from IR thermography. (d) and (e) q_{lim} poloidal profiles at the centre ($\phi = 1:06$) and on the left wing ($\phi = 1:04$) from the map (b) and (c) respectively.

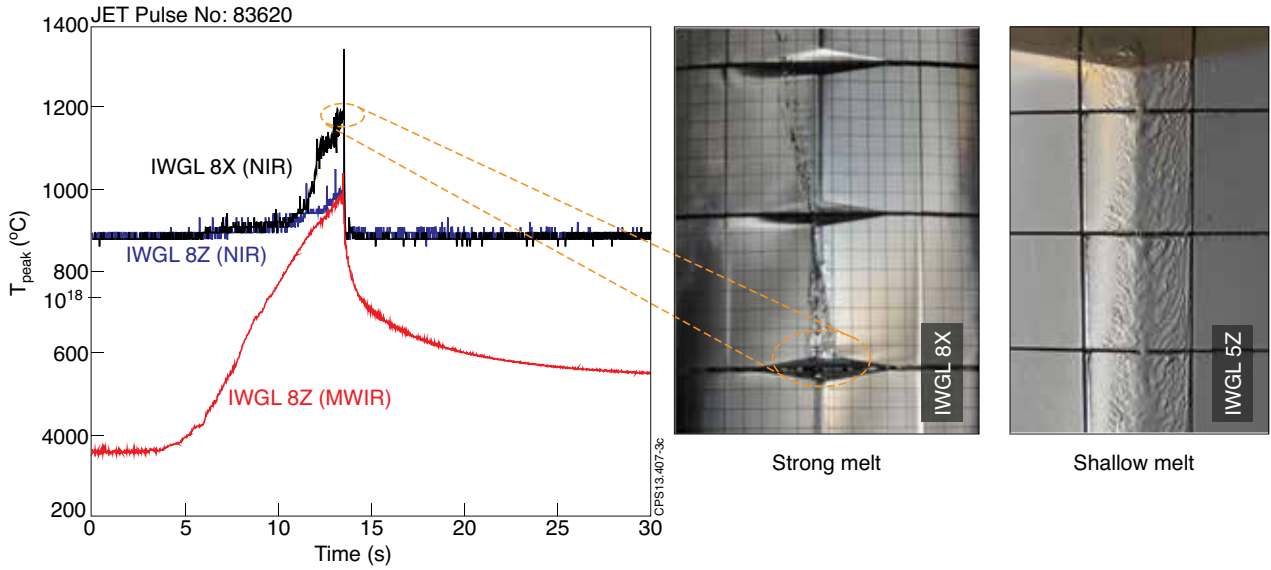


Figure 3: (a) Peak temperature, T_{peak} measured on the IWGL 8Z by the MWIR camera (red) and by the PIW (NIR, 1m) camera (blue), and on the IWGL 8X by the PIW camera (black). (b) Picture of the melt damage that occurred during JET Pulse No: 83620 on the IWGL 8X. The melt damage coincides with the plasma contact point.

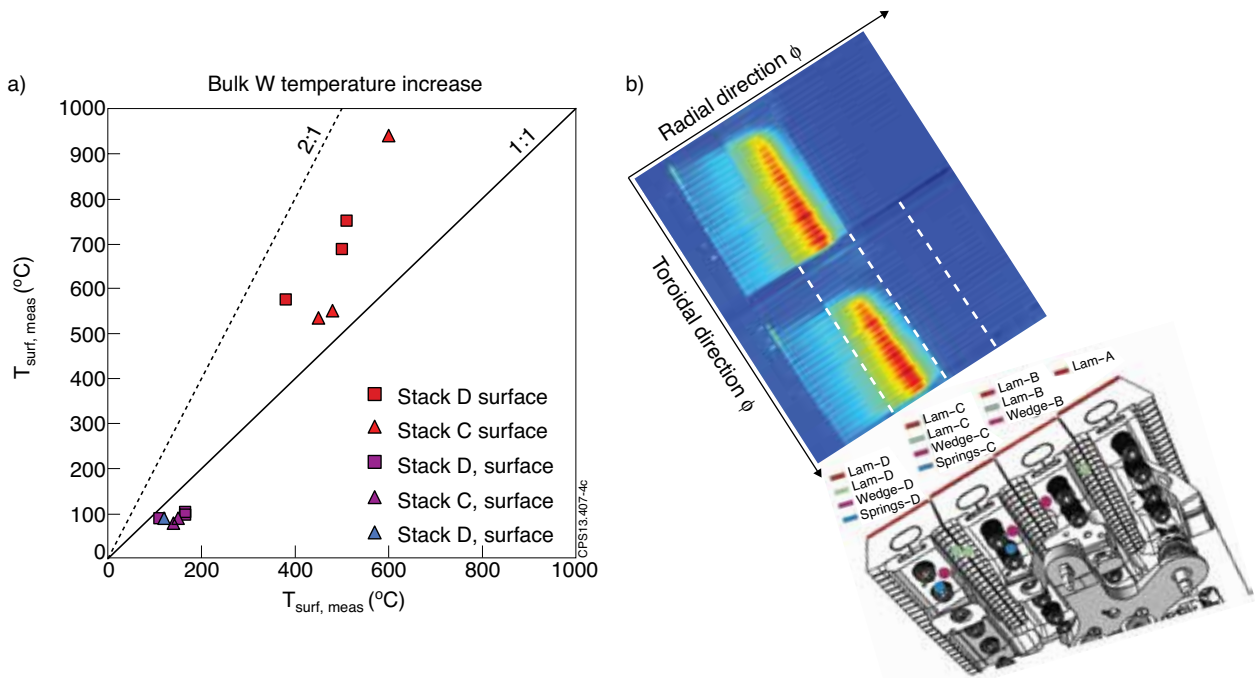


Figure 4: (a) Temperature increase measured in the bulk W tile as a function of that predicted by the GTM code. Triangles and squares indicate which stack the measurement comes from. The colours indicate where the measurement has been taken: on the surface, T_{surf} , (red) at the wedge, T_{wedge} , (purple) or on the springs, T_{spring} (blue). (b) Illustration of the instrumentation of the tile for temperature measurement. T_{surf} can be measured at any point on the tile using IR images. T_{wedge} and T_{spring} are measured with thermocouples at the position indicated by the purple and blue dots respectively.